ORIGINAL RESEARCH ■ GENITOURINARY IMAGING

Radiology

Uterine Artery Embolization:
Optimization with Preprocedural Prediction of the Best Tube Angle Obliquity by Using 3D-Reconstructed Contrast-enhanced MR Angiography[1]

Nagy N. N. Naguib, MSc
Nour-Eldin A. Nour-Eldin, MSc
Thomas Lehnert, MD
Renate M. Hammerstingl, MD
Huedayi Korkusuz, MD
Katrin Eichler, MD
Stephan Zangos, MD
Thomas J. Vogl, MD

Purpose: To evaluate the effect of preprocedural prediction of the best tube angle obliquity for visualization of the uterine artery origin by using three-dimensional (3D)–reconstructed contrast material–enhanced magnetic resonance (MR) angiography on the radiation dose, fluoroscopy time, and contrast medium volume during uterine artery embolization (UAE).

Materials and Methods: The study was approved by the institutional review board. Informed consent was obtained. The prospective study included 20 consecutive prospective patients (age range, 37–56 years) for whom preprocedural prediction of the best tube angle obliquity was determined by using 3D-reconstructed contrast-enhanced MR angiography; the best tube angle obliquity was provided to the interventionist. Three-dimensional reconstruction was performed by using an application of the angiographic unit. The radiation dose, fluoroscopy time, and contrast medium volume for those patients were compared with those data in 20 retrospectively assessed control patients (age range, 39–56 years) from the prior 20 procedures performed by the same interventionist.

Results: Tube angle prediction resulted in a significant reduction in the radiation dose utilized ($P < .001$), fluoroscopy time ($P = .002$), and contrast medium volume ($P < .001$) for the sample patients compared with those for the control patients. Overall radiation dose was reduced from a mean of 11 044 µGy per square meter to a mean of 4172.5 µGy per square meter. Fluoroscopy time was reduced from a mean of 15 minutes 30 seconds to 8 minutes 49 seconds. Contrast medium volume was reduced from a mean of 135 mL to 75 mL.

Conclusion: Preprocedural prediction of the best tube angle obliquity for visualization of the origin of the uterine artery by using 3D-reconstructed contrast-enhanced MR angiography results in significant reductions in radiation dose, fluoroscopy time, and contrast medium volume during UAE.

© RSNA, 2009

© RSNA, 2009

Uterine artery embolization (UAE) is a minimally invasive therapy for uterine leiomyomata that represents an alternative to hysterectomy and myomectomy (1–5). During the past decade, UAE has been established as a safe and effective first-line therapy for the treatment of symptomatic fibroids in premenopausal women (6–10). Almost all patients who undergo UAE procedures are women of childbearing age, and because UAE requires fluoroscopic and angiographic imaging, the radiation exposure may affect the function of the ovaries (11). Because the patient is exposed to ionizing radiation during UAE, all procedures and radiation exposure should be governed by the principle of as low as reasonably achievable (12).

Several previous studies suggest methods for reducing ovarian exposure and overall radiation dose during the procedure, such as the use of elective bilateral femoral puncture (13), pulsed fluoroscopy instead of nonpulsed fluoroscopy, a well-collimated field of view, and nonmagnified instead of magnified views and reduced utilization of oblique views when possible (14). In addition, other studies (15) showed that there is no standard angle of obliquity for the visualization of the origin of the uterine artery for its catheterization.

Our study was designed to evaluate the effect of preprocedural prediction of the best tube angle obliquity for visualization of the origin of the uterine artery by using three-dimensional (3D)–reconstructed contrast material–enhanced magnetic resonance (MR) angiography on the radiation dose, fluoroscopy time, and contrast medium volume during the procedure.

Materials and Methods

Patient Selection and Study Design

The institutional review board approved the study, and written informed consent was obtained. (The preprinted consent form included patient approval for the UAE procedure and contrast-enhanced MR imaging and MR angiography and the anonymous utilization of the images and data for research purposes. In addition, the 3D reconstruction process was explained to the patients of the prospective arm.) Forty consecutive patients (20 prospective patients and 20 retrospective control patients) were included. The Table summarizes the demographic data, uterine volume, and overall fibroid volume for both the control and sample groups. Patient symptoms included abnormal uterine bleeding ($n = 38$), bulk-related symptoms ($n = 22$), pain ($n = 13$), or a combination of symptoms ($n = 32$). All patients expressed a desire to avoid surgical treatment and were extensively counseled as to the known risks and benefits of UAE and to the alternatives to UAE.

Radiation dose, fluoroscopy time, and contrast medium volume for the 20 sample patients were compared with those for the 20 control patients. In the 20 sample patients, contrast-enhanced MR angiography was performed before UAE and was used to predict the best tube angle obliquity for visualization of the uterine artery origin by using 3D reconstruction of the MR angiographic series. The 20 control patients were the last 20 consecutive patients who had undergone UAE performed by the same interventionist before the prospective portion of the study (for whom no angle was predicted). They represented the retrospective arm of the study, and their data were used to compare and test the effect of angle prediction on radiation dose, fluoroscopy time, and contrast medium volume.

A single interventionist (T.J.V., with more than 15 years of experience in interventional radiology and who had performed more than 200 UAE procedures before the beginning of the study) performed all UAE procedures. The same angiographic parameters were used in all 40 patients. The angiographic series for procedure documentation was acquired according to the published guidelines of the Society of Interventional Radiology (16). These include the acquisition of a single-mapping internal iliac artery angiogram for each side with the suggested oblique view, an immediate preembolization uterine artery angiogram, and an immediate postembolization uterine artery angiogram.

MR Imaging and Image Reconstruction Technique

Contrast-enhanced MR angiography is performed in our institute as a routine study prior to UAE. Contrast-enhanced MR angiography was performed with a 1.5-T MR imaging system (Magnetom Avanto; Siemens

Advances in Knowledge

- Preprocedural prediction of the best tube angle obliquity for visualization of the origin of the uterine artery significantly reduces fluoroscopy time, radiation dose, and contrast medium volume during uterine artery embolization (UAE).
- Three-dimensional reconstruction improves the diagnostic utilization of contrast-enhanced MR angiographic images.

Implications for Patient Care

- Patients undergoing UAE can receive a lower radiation dose and a lower iodinated contrast material dose with preprocedural MR angiography for determination of the optimal tube obliquity.
- Reduction of radiation dose and fluoroscopy time reduces the hazardous radiation exposure to patients.
- Reduction of the contrast medium volume used during the procedure reduces the contrast medium burden on the kidneys.

Medical Systems, Erlangen, Germany). A body-array coil was used to cover the volume of interest. Gradient-echo scout images (repetition time msec/echo time msec, 15/5; flip angle, 40°; section thickness, 10 mm; matrix, 128 × 256; field of view, 40 cm) were obtained in the axial, coronal, and sagittal planes. T2-weighted single-shot turbo spin-echo MR images (4000/95; flip angle, 150°; section thickness, 6 mm; matrix, 128 × 256; field of view, 35 cm) were obtained in the sagittal direction. An unenhanced 3D fast low-angle shot sequence (3.66/1.28; flip angle, 25°; section thickness, 1.2 mm; matrix, 128 × 512; field of view, 35 cm; voxel dimensions, 1.2 × 0.9 × 1.0 mm; imaging duration, 21 seconds) in the coronal section orientation was performed; this sequence utilizes both zero padding and partial Fourier techniques.

For the determination of the travel time for contrast material from the injection site to the pelvic vessels, a test bolus technique was used. Two milliliters of gadopentetate dimeglumine (Magnevist; Schering, Berlin, Germany) was used for this purpose. On the basis of circulation time, contrast-enhanced MR angiography was performed during the end-inspiratory phase, and the contrast material was intravenously administered (0.1 mL per kilogram of body weight followed by 20 mL normal saline) by using a power injector (Spectris; Medrad, Pittsburgh, Pa) with a flow rate of 3 mL/sec. Contrast-enhanced MR angiography was performed with a 3D fast low-angle shot sequence (3.66/1.28; flip angle, 25°; section thickness, 1.2 mm; matrix, 128 × 512; field of view, 35 cm; voxel dimensions, 1.2 × 0.9 × 1.0 mm; imaging duration, 63 seconds) in the arterial and venous phases. Both the unenhanced and the contrast-enhanced 3D fast low-angle shot acquisitions were obtained with breath holding. (For the postcontrast sequence, the patient was asked to hold her breath as long as she could and then to release it gradually.) Subtracted images in the arterial phase were loaded into an ap-plication (Inspace) of the angiography console (Axiom Artis; Siemens Medical Systems), and a 3D-reconstructed volume-rendered view of the pelvic arterial tree was obtained.

Image Evaluation and Angle Prediction

All MR images were assessed in consensus by two radiologists (N.N.N.N. and S.Z., with more than 8 and 15 years of experience, respectively, in pelvic MR imaging). The two reviewers performed all the 3D reconstructions together in consensus and used the 3D model for their assessment. The uterine artery with its characteristic tortuous course was identified and traced backward to its origin, where the 3D-reconstructed figure of the pelvic arterial tree was slowly rotated in both directions in an attempt to visually identify the best obliquity that clearly delineated its origin. In all 20 sample patients, the uterine artery was clearly identified on the 3D reconstructed model and could be successfully traced to its origin. In all cases, the uterine artery originated from the anterior division of the internal iliac artery. The application (Inspace) provides the C-arm obliquity angle that corresponds to the rotated 3D figure (Fig 1a). The ability of the C-arm to swing was also kept in consideration. (Applicability of the chosen angle was also kept in consideration.) Two angles were suggested for each patient—one representing the best angle for visualization of the left uterine artery origin and the second representing the best angle for visualization of the right uterine artery origin. All angles provided in our study clearly demonstrated the origin of the uterine artery without the need for further caudal or cephalic an-gulations. The angles were provided to the interventionist, who was asked to utilize the provided angles of obliquity for better visualization of the uterine artery origin during the procedure but who was blinded to the parameters being investigated and the aims of the study to reduce radiation dose and contrast medium dose.

UAE Procedure

All embolization procedures were technically successful, and both uterine arteries were successfully embolized until stasis was observed. Both uterine arteries were successfully catheterized in all patients, and the immediate postintervention contrast-enhanced MR image showed complete nonenhancement of all fibroids.

All UAE procedures (n = 40) were performed by using a unilateral right femoral arterial approach and were performed with angiographic guidance (Axiom Artis) by using nonpulsed fluoroscopy. After local anesthesia was induced, the femoral artery was punctured by using the Seldinger technique, and a 5-F sheath (Terumo, Tokyo, Japan) was inserted. A 5-F pigtail catheter (Boston Scientific, Annacotty, Ireland) with a hydrophilic polymer–coated 0.032-inch guidewire (Radifocus; Terumo) was inserted for the crossover to the contralateral common iliac artery. The 5-F pigtail catheter was then exchanged over the guidewire with a 4-F catheter (Cobra C2; Terumo), which was then manipulated and used for catheterization of the contralateral uterine artery.

Embolization was performed by using microspheres (Bead Block; Terumo) 500–700 μm in size. The currently rec-

Demographic Data, Uterine Volume, and Fibroid Volume in 40 Patients			
Parameter	Control Group (n = 20)	Sample Group (n = 20)	P Value
Age (y)	46.2 ± 3.87 (39–56)	46 ± 5.12 (37–56)	.88
Patient weight (kg)	67.9 ± 7.13 (55–80)	67.45 ± 7.78 (57–82)	.85
Uterine volume (mL)	332.4 ± 194.2 (117.5–851)	387.9 ± 184 (138.7–851)	.4
Fibroid volume (mL)	122.7 ± 108.4 (22–375.4)	115.1 ± 98.2 (18.5–347.6)	.77

Note.—Data are means ± standard deviations, with ranges in parentheses.

ommended size for microspheres for embolization is 700–900 μm; however, this study was performed before the current recommendations were published by Kroencke et al (17). For the catheterization of the ipsilateral internal iliac artery, a 5-F catheter (Sidewinder 1; Terumo) was used. Catheterization of the ipsilateral uterine artery was achieved by using the Sidewinder catheter alone in 17 patients (nine sample patients and eight control patients), while a microcatheter (Renegade; Boston Scientific, Cork, Ireland) and a 0.014-inch microguidewire (Transend; Boston Scientific, Miami, Fla) were needed in the remaining 23 patients (11 sample patients and 12 control patients). The embolization procedure was monitored by using the direct anteroposterior view of the pelvis to avoid possible overexposure of the ovaries associated with oblique views of the pelvis, which were used only during catheterization of the uterine artery. Observation of stasis in the uterine artery was considered to be the end point of embolization. After the procedure, the patient was transferred to the ward for observation, and pain was managed by using intravenous analgesics.

Data Collection and Statistical Analysis

The uterine volume and overall fibroid volume were obtained from the MR imaging study performed before the procedure and were calculated by using the formula for ellipsoid volume (height × length × width × 0.523). Fluoroscopy time and radiation dose were obtained from the angiography machine at the end of the procedure for sample patients and from patient records for the control patients. The overall radiation dose was subdivided into radiation dose during fluoroscopy and radiation dose during digital subtraction angiographic (DSA) acquisition. Volume of contrast medium injected in the patient was recorded.

Radiation dose, fluoroscopy time, and contrast medium volume during UAE for the sample patients were compared with the same data for the control patients. The difference in data between the control and sample groups was tested by using the Student t test (for age, weight, and uterine and overall fibroid volume) and the Welch t test (for radiation dose, fluoroscopy time, and contrast medium volume), and the data were graphically displayed by using box plots. The differences in radiation dose, fluoroscopy time, and contrast medium volume in relation to the usage or nonusage of a microcatheter was also tested by using the Student t test. $P < .05$ was considered to indicate a statistically significant difference. All statistical evaluations were performed by using software (BiAS for Windows; Epsilon Publisher, Darmstadt, Germany).

Results

The mean volume of embolization material (microspheres) used was 5.9 mL ± 2.634 (standard deviation) (range, 2–12 mL) among the control patients and 6 mL ± 2.902 (range, 2–14 mL) among the sample patients. No statistically significant difference was noted between the control and sample patients with regard to the amount of embolization material used ($P = .92$).

Predicted Angle

The predicted angle of tube obliquity provided to the interventionist before the

Figure 1

Figure 1:   Images in 44-year-old woman. **(a)** Three-dimensional–reconstructed contrast-enhanced MR angiographic image from the preembolization study. The model was rotated to a 24° left obliquity for demonstration of the origin (arrow) of the right uterine artery *(U)* (routine oblique view). Upper right corner of the image shows the corresponding C-arm position and the obliquity angle (24° left oblique). **(b)** DSA image in the same patient shows the corresponding angiographic projection and clear demonstration of the origin (arrow) of the right uterine artery *(U)*. Additional arteries visualized include the common iliac *(CI)*, external iliac *(EI)*, inferior gluteal *(IG)*, internal iliac *(II)*, internal pudendal *(IP)*, obturator *(O)*, superior gluteal *(SG)*, and superior vesical *(SV)*.
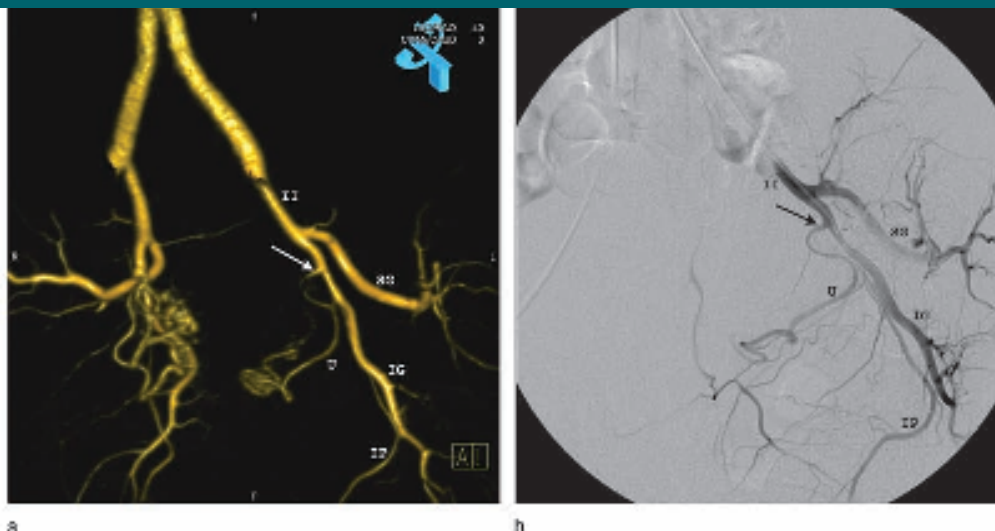
Figure 2

Figure 2: Images in 42-year-old woman. **(a)** Three-dimensional–reconstructed contrast-enhanced MR angiographic image from the preembolization study. The model was rotated to a 40° left obliquity (contrary to the usual right oblique view used for the left uterine artery) for demonstration of the origin (arrow) of the left uterine artery *(U)*. Upper right corner of the image shows the corresponding C-arm position and the obliquity angle (40° left oblique). **(b)** DSA image in the same patient shows the corresponding angiographic projection and clear demonstration of the origin (arrow) of the left uterine artery *(U)*. Additional arteries visualized include the inferior gluteal *(IG),* internal iliac *(II),* internal pudendal *(IP),* and superior gluteal *(SG).*

procedure (Fig 1a) was the same as the actual angle (Fig 1b) used during the procedure for the visualization of the origin of the uterine artery (ie, all angles suggested in the current study were correctly predicted). The preprocedural predicted angle for the left side was between 45° right (ie, the intensifying screen was moved toward the right side of the patient) and 45° left (mean, 16.25° right ± 20.7). For the right side, the predicted angle was between 50° left and 50° right (mean, 13.75° left ± 27.2). For visualization of the left uterine artery origin, the routine right anterior oblique view was used in 15 of 20 patients (angle range, 10°–45°), while the left anterior oblique view (Fig 2) was used in five (25%) patients (angle range, 9°–45°). For visualization of the right uterine artery origin, the routine left anterior oblique view was used in 15 of 20 patients (angle range, 13°–50°), while the right anterior oblique view was used in four (20%) patients (angle range, 10°–50°). In one (5%) patient, the direct anteroposterior view was used.

Radiation Dose

Preprocedural prediction of the best tube angle obliquity resulted in a significant reduction in the overall radiation dose utilized during UAE ($P < .001$) from a mean radiation dose of 11 044 μGy per square meter ± 4036.9 (range, 6295.8–17 476 μGy per square meter) for the control patients to a mean radiation dose of 4172.5 μGy per square meter ± 1555.76 (range, 1058.5–7577
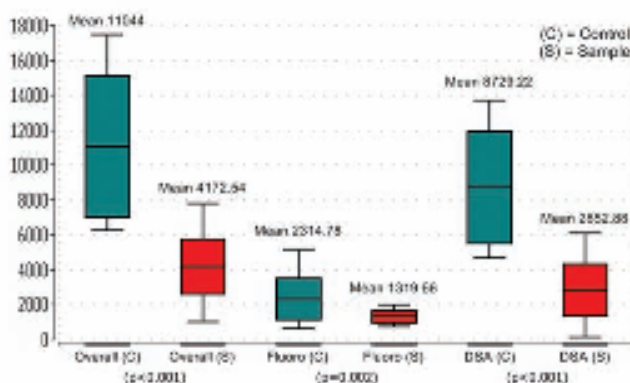
Figure 3

Figure 3: Box plot shows significantly reduced overall radiation dose ($P < .001$), fluoroscopy *(Fluoro)*-related radiation dose ($P = .002$), and DSA-related radiation dose ($P < .001$) during UAE in sample patients compared with control patients. Vertical axis is radiation dose in micrograys per square meter. Middle line = mean, box = standard deviation, whiskers = minimum and maximum values.

μGy per square meter) for the sample patients (Fig 3). Thus, the mean overall radiation dose was reduced by about 62% for the sample patients compared with the control patients.

Mean radiation dose related to fluoroscopy was reduced by 43%; the reduction was statistically significant ($P =$

.002). Mean radiation dose related to DSA acquisition was reduced by 67% ($P < .001$).

No statistically significant difference was noted regarding the radiation dose between patients in whom a microcatheter was used and patients in whom no microcatheter was used ($P = .20$).

Fluoroscopy Time

Fluoroscopy time was significantly reduced by 43% ($P = .002$) from a mean of 15 minutes 30 seconds ± 7 minutes
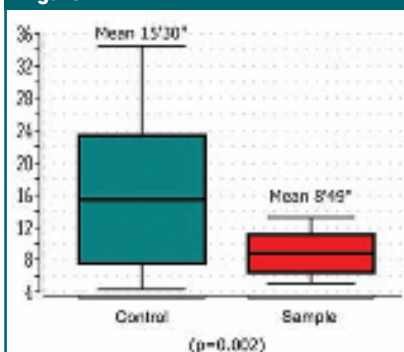
Figure 4

Figure 4: Box plot shows significantly ($P = .002$) reduced fluoroscopy time during UAE in sample patients compared with control patients. Vertical axis is time in minutes. Middle line = mean, box = standard deviation, whiskers = minimum and maximum values.
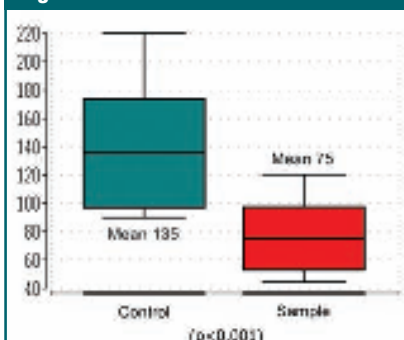
Figure 5

Figure 5: Box plot shows significantly ($P < .001$) reduced contrast medium volume used during UAE in sample patients compared with control patients. Vertical axis is contrast material volume in milliliters. Middle line = mean, box = standard deviation, whiskers = minimum and maximum values.

54 seconds (range, 4 minutes 24 seconds to 34 minutes) in the control group to a mean of 8 minutes 49 seconds ± 2 minutes 18 seconds (range, 5 minutes 6 seconds to 13 minutes 30 seconds) in the sample group (Fig 4).

No statistically significant difference was noted regarding the fluoroscopy time between patients in whom a microcatheter was used and patients in whom no microcatheter was used ($P = .37$).

Contrast Medium Volume

Contrast medium volume was significantly reduced by 44% ($P < .001$) from a mean of 135 mL ± 38.2 (range, 90–220 mL) for the control patients to a mean of 75 mL ± 22.1 (range, 45–120 mL) for the sample patients (Fig 5).

No statistically significant difference was noted regarding the contrast medium volume between patients in whom a microcatheter was used and patients in whom no microcatheter was used ($P = .65$).

Discussion

Almost all patients who undergo UAE procedures are women of childbearing age, and limitation of radiation dose is important (14). On the basis of this fact, several previous studies (18,19) were performed to reduce the ovarian radiation dose during UAE by using a smaller field of view and better collimation, by using nonmagnified views instead of magnified views, and with reasonable use of oblique views that place the ovaries in the direct line of the radiation beam.

In addition, the amount of contrast medium used in interventional procedures constitutes a burden on renal function (20–22).

Our current study was conducted in an attempt to reduce the radiation dose and contrast medium volume utilized during UAE by providing the interventionist with a single angle of tube obliquity for each side tailored to each patient that best demonstrates the origin of the uterine artery without using ionizing radiation.

We demonstrated that angle prediction significantly reduces radiation dose, fluoroscopy time, and contrast medium

volume during the UAE procedure. In addition, we observed that no standard angle can be recommended for all patients, and the angle should be tailored for each patient. Even the usual direction of tube obliquity (right oblique view for the left artery and left oblique view for the right artery) may fail to demonstrate the origin, regardless of the obliquity angle used in this direction. However, the standard direction of obliquity still represents 75% of the angulations used in the current study.

The overall radiation dose was reduced by 62%, while the reduction in fluoroscopy time was 43%. Fluoroscopy time is composed of three parts: The first part represents time spent searching for the origin of the artery and the best angle of obliquity to demonstrate the origin. The second part is time required to negotiate and catheterize the artery, and this part becomes shorter through practice and experience. The third part is time spent monitoring the embolization procedure, and this part is relatively difficult to change. The reduction in fluoroscopy time achieved in our study was likely related to reducing the first part.

Similarly, the radiation dose utilized represents the radiation required during fluoroscopy and during DSA series acquisition. Because we provided the interventionist with a single obliquity for each uterine artery that best demonstrated its origin, the need for several DSA series with different obliquities to clearly demonstrate the origin was reduced. Therefore, our results demonstrate a larger reduction of the radiation dose utilized at DSA (67%) than the reduction noted in relation to fluoroscopy radiation dose (43%).

In their study on a model, Dietrich et al (23) attempted to reduce the fluoroscopy time by using a magnetic navigation system; thus, they attempted to manipulate the time required for catheterization of the artery in a way other than improving the experience of the interventionist. However, no further work was published regarding the use of such a technique in practice.

Bratby et al (13) demonstrated a 23% reduction in the mean fluoroscopy time

and about a 30% reduction in the mean radiation dose used during the procedure through the utilization of elective bilateral femoral arterial puncture, sequential catheterization of both uterine arteries, and simultaneous injection of the embolizing material.

Another way of reducing the radiation dose was presented by Nikolic et al (14), who concluded that it is possible to achieve about a 50% radiation dose reduction by using pulsed fluoroscopy instead of continuous fluoroscopy. In our study, we used nonpulsed fluoroscopy. The use of pulsed fluoroscopy can provide further reduction in patient radiation dose; however, we did not try to interfere with the interventionist's decisions, especially because we wanted him to perform the prospective part in exactly the same manner as the retrospective part to eliminate any possible bias related to the machine parameters used. Other measures that can be utilized to reduce the radiation dose and procedure time include the utilization of a single catheter to perform contralateral and ipsilateral embolization of both uterine arteries (24).

Bucek et al (15) used 3D rotational DSA to predict the best tube angle obliquity and concluded that there is no standard angle of obliquity that can be recommended for all patients and that there was no statistically significant reduction in the fluoroscopy time, radiation dose, or contrast medium volume when 3D rotational DSA was used for obliquity angle prediction. Reasons for discrepancy with our findings include the following: First, the utilization of DSA itself constituted a radiation exposure that required contrast medium injection, which adds to the overall radiation and contrast medium dose used. Second, they compared only eight patients who had huge fibroids and complex anatomy with 48 patients with standard angiographic findings; thus, there was a possible bias in patient selection. In addition, large fibroids displace the uterine arteries and make them difficult to catheterize even if the origin is well demonstrated, thus adding to the overall fluoroscopy time, radiation dose, and contrast medium volume. Finally, we believe that the improvement in software provided by manufacturers over the years

(4 years since they published their results) could have improved the quality and resolution of images, leading to increased utility.

A limitation of our study was that it was nonrandomized. Our initial results obtained after the first patients (two pilot cases) constituted an ethical problem because it was clear that there was radiation dose reduction, which rendered it at least partially unethical not to use the technique for some patients if a randomized study was to be performed. A second limitation was the utilization of a microcatheter in some patients, which is associated with increased radiation during delivery of embolization particles; however, in our study, no statistically significant difference was noted in association with microcatheter usage regarding the radiation dose, fluoroscopy time, and contrast medium volume.

We regard the current study as a step on a long road of utilization of 3D reconstruction in interventional radiology. Further studies aiming to utilize such capabilities of 3D images in determining ovarian supply of uterine fibroids and to compare axial versus coronal 3D contrast-enhanced MR angiograms are required. In addition, 3D MR angiography has been shown to reveal anatomic details and variations of the uterine arteries (25).

We conclude that it is possible to achieve significant reduction in radiation dose, fluoroscopy time, and contrast medium volume during UAE through preprocedural prediction of the best tube angle obliquity by using 3D-reconstructed contrast-enhanced MR angiography. Thus, in addition to its well-documented value as a preprocedural method of evaluation, MR angiography allowed the use of 3D reconstruction for angle prediction; thus, it proved to be of practical value during the procedure.

References

1. Subramanian S, Spies JB. Uterine artery embolization for leiomyomata: resource use and cost estimation. J Vasc Interv Radiol 2001; 12:571–574.

2. Ravina JH, Herbreteau D, Ciraru-Vigneron N, et al. Arterial embolization to treat uterine myomata. Lancet 1995;346:671–672.

3. Goodwin SC, Wong GC. Uterine artery embolization for uterine fibroids: a radiologist's perspective. Clin Obstet Gynecol 2001;44:412–424.

4. Sterling KM, Siskin GP, Ponturo MM, Mandato K, Rholl KS, Cooper JM. A multi-center study evaluating the use of gelfoam only for uterine artery embolization for symptomatic leiomyomata [abstr]. J Vasc Interv Radiol 2002;13(suppl):S19.

5. Katsumori T, Kasahara T, Akazawa K. Long-term outcomes of uterine artery embolization using gelatin sponge particles alone for symptomatic fibroids. AJR Am J Roentgenol 2006;186:848–854.

6. Chrisman HB, Minocha J, Ryu RK, Vogelzang RL, Nikolaidis P, Omary RA. Uterine artery embolization: a treatment option for symptomatic fibroids in postmenopausal women. J Vasc Interv Radiol 2007;18:451–454.

7. Worthington-Kirsch RL, Popky GL, Hutchins FL. Uterine arterial embolization for the management of leiomyomas: quality of life assessment and clinical response. Radiology 1998; 208:625–629.

8. Lipman JC. Uterine artery embolization for the treatment of symptomatic uterine fibroids: a review. Appl Radiol 2000;29:15–20.

9. Machan L, Goodwin S, Worthington-Kirsch R, Spies R. Fibroid embolization: periprocedural care. Semin Interv Radiol 2000;17:247–254.

10. Bucek RA, Puchner S, Lammer J. Mid- and long-term quality-of-life assessment in patients undergoing uterine fibroid embolization. AJR Am J Roentgenol 2006;186:877–882.

11. Spies JB, Roth AR, Gonsalves SM, Murphy-Skrzyniarz KM. Ovarian function after uterine artery embolization for leiomyomata: assessment with use of serum follicle stimulating hormone assay. J Vasc Interv Radiol 2001;12:437–442.

12. Andrews RT, Spies JB, Sacks D, et al. Patient care and uterine artery embolization for leiomyomata. J Vasc Interv Radiol 2004; 15:115–120.

13. Bratby MJ, Ramachandran N, Sheppard N, Kyriou J, Munneke GM, Belli AM. Prospective study of elective bilateral versus unilateral femoral arterial puncture for uterine artery embolization. Cardiovasc Intervent Radiol 2007;30:1139–1143.

14. Nikolic B, Spies JB, Campbell L, Walsh SM, Abbara S, Lundsten MJ. Uterine artery embolization: reduced radiation with

Radiology

refined technique. J Vasc Interv Radiol 2001;12:39–44.

15. Bucek RA, Reiter M, Dirisamer A, Kettenbach J, Lammer J. Three-dimensional digital rotation angiography for embolization therapy of uterine leiomyomas: first results [in German]. Rofo 2004;176:1001–1004.

16. Spies J, Niedzwiecki G, Goodwin S, et al. Training standards for physicians performing uterine artery embolization for leiomyomata. J Vasc Interv Radiol 2001;12:19–21.

17. Kroencke TJ, Scheurig C, Lampmann LE, et al. Acrylamido polyvinyl alcohol microspheres for uterine artery embolization: 12-month clinical and MR imaging results. J Vasc Interv Radiol 2008;19:47–57.

18. Andrews RT, Brown PH. Uterine arterial embolization: factors influencing patient ra-diation exposure. Radiology 2000;217:713–722.

19. Nikolic B, Abbara S, Levy E, et al. Influence of radiographic technique and equipment on absorbed ovarian dose associated with uterine artery embolization. J Vasc Interv Radiol 2000;11:1173–1178.

20. Rudnick MR, Goldfarb S, Wexler L, et al. Nephrotoxicity of ionic and nonionic contrast media in 1196 patients: a randomized trial. Kidney Int 1995;47:254–261.

21. Schwab SJ, Hlatky MA, Piper KS, et al. Contrast nephrotoxicity: a randomized controlled trial of a nonionic and ionic radiographic contrast agent. N Engl J Med 1989;320:149–153.

22. Parfrey PS, Griffiths SM, Barrett BJ, et al. Contrast material-induced renal failure in patients with diabetes mellitus, renal insufficiency, or both: a prospective controlled study. N Engl J Med 1989;320:143–149.

23. Dietrich T, Kleen M, Killmann R, et al. Evaluation of magnetic navigation in an in vitro model of uterine artery embolization. J Vasc Interv Radiol 2004;15:1457–1462.

24. Pelage JP, Soyer P, Le Dref O, et al. Uterine arteries: bilateral catheterization with a single femoral approach and a single 5-F catheter—technical note. Radiology 1999; 210:573–575.

25. Naguib NN, Nour-Eldin NE, Hammerstingl RM, et al. Three-dimensional reconstructed contrast-enhanced MR angiography for internal iliac artery branch visualization before uterine artery embolization. J Vasc Interv Radiol 2008;19:1569–1575.